Antecedent Atmospheric Conditions Related to Squall-Line Initiation over the Northern Coast of Brazil in July

FERNANDO PEREIRA DE OLIVEIRA

Instituto Nacional de Pesquisas Espaciais, Centro de Previsão de Tempo e Estudos Climáticos, Cachoeira Paulista, Brazil

MARCOS DAISUKE OYAMA

Instituto de Aeronáutica e Espaço, Divisão de Ciências Atmosféricas, São José dos Campos, Brazil

(Manuscript received 30 September 2014, in final form 1 June 2015)

ABSTRACT

The antecedent atmospheric conditions at midmorning (1200 UTC or 0900 LST) related to subsequent squall-line (SL) initiation in the late afternoon or early evening over the northern coast of Brazil (NCB) were obtained for a specific month (July) when the SL initiation is independent of the strong synoptic forcing related to the intertropical convergence zone. The cases of SL and sparse deep convection in the late afternoon or early evening over the NCB were identified both objectively and subjectively, and grouped into either the SL category (SLC) or the no-convection category (NOC). For the central area of the NCB, the vertical profiles at midmorning for SLC and NOC, computed from radiosonde and ERA-Interim data spanning 9 years (2004–12), were compared. By focusing on the significant differences for both datasets, it was found that two midmorning conditions are favorable to SL initiation in July: a moister layer between 850 and 350 hPa, and a northeasterly flow at 350 hPa. These regional conditions are part of a larger-scale pattern: moister (drier) conditions over the whole NCB (southeastern South America) at 700 hPa and more intense anticyclonic circulation over the Atlantic Ocean close to northeastern Brazil at 350 hPa. The paper's findings have the potential to aid weather forecasting activities, such as those focused on the prediction of SL-related precipitation 6–12 h ahead.

1. Introduction

Along the northern coast of Brazil (NCB), the precipitation regime is strongly related to the latitudinal migration of the intertropical convergence zone (ITCZ; Molion and Bernardo 2002; Reboita et al. 2010). Maximum (minimum) precipitation occurs in the austral autumn (spring), when the ITCZ reaches its southernmost (northernmost) position. Another important meteorological system, responsible for large precipitation amounts in the NCB, is the squall line (SL). The general features of SLs initiated over the NCB have been described in numerous studies (Kousky 1980; Cavalcanti 1982; Cohen et al. 1989, 2009; Greco et al. 1990; Garstang et al. 1994; Barros 2008; Barros and Oyama 2010). SLs are mesoscale convective systems that initiate in the late afternoon or early evening, when cumulonimbus clouds upscale and become organized as linear bands of cloudiness over the NCB and parallel to the coastline (Fig. 1a). The sea-breeze circulation is regarded as an important process during SL initiation. The average SL dimensions are 1400 km (length along the coastline direction) × 170 km (width) × 14 km (height). SLs occur all year round (~10 cases per month) over the NCB, but higher frequency is found in the austral autumn, when the ITCZ directly affects the NCB, providing a large-scale low-level convergence environment (favorable to deep convection) in which SLs initiate, triggered by the sea-breeze circulation.

After the initiation, the SLs propagate inland as a linear multicell storm (Houze 2004; Garstang et al. 1994), with low-level convergence and upper-level divergence in the convective portion, and midlevel convergence with low- and upper-level divergence in the stratiform portion. In about half of the cases (~55%), propagation is small, and the SLs become practically confined to the coast and last for ~10 h; in the remainder

Corresponding author address: Marcos Oyama, Praça Marechal Eduardo Gomes, 50, Vila das Acácias, 12228-904 São José dos Campos, SP, Brazil.
E-mail: marcos.oyama@ymail.com

DOI: 10.1175/WAF-D-14-00120.1

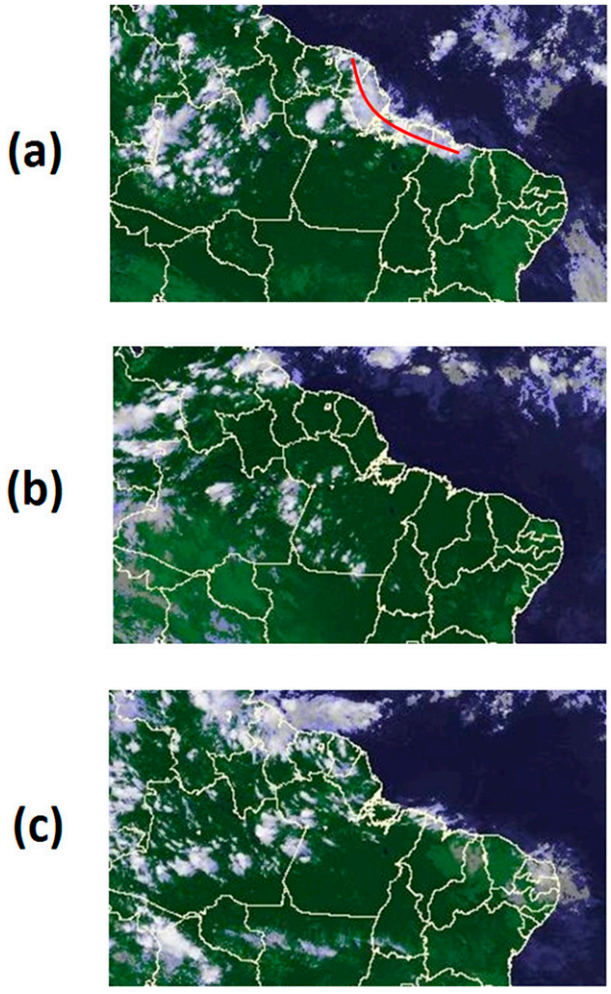

FIG. 1. Infrared satellite images (from CPTEC, Brazil) illustrating the convection categories in the NCB in July: (a) SLC (2130 UTC 6 Jul 2008), where the SL is indicated by the red line; (b) NOC (2100 UTC 25 Jul 2009); and (c) the coastal convection category (2100 UTC 6 Jul 2009).

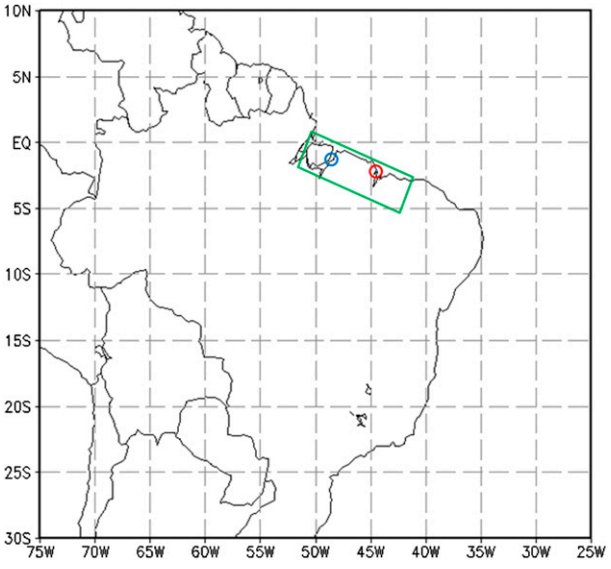

FIG. 2. Location of CLA (red circle) and Belém (blue circle). The objective method searches for convective systems that take place over the box area (green) in the NCB.

of cases (~45%), the SLs propagate far inland, last for ~20 h and can reach central and western Amazonia (Cohen et al. 2009).

Given an SL initiation, the extent of its propagation depends on the features of the vertical wind profile: in general, propagation is favored by a deep and intense low-level jet during midmorning (Cohen et al. 1995; Alcântara et al. 2011). One issue that has not been addressed by previous studies is whether there are particular conditions of the atmospheric environment during midmorning that favor the initiation of SLs in the subsequent late afternoon or early evening. The motivation for this point is the possibility of predicting the occurrence of SL-related precipitation 6–12 h ahead, from the midmorning (1200 UTC or 0900 LST) radiosonde data collected at localities in NCB. Here, the issue of antecedent conditions related to the initiation of SLs is addressed for a specific region within the NCB—the Alcântara Launch Center [Centro de Lançamento de Alcântara (CLA)] region (Fig. 2)—and for a specific month, July.

The CLA is located in the central portion of NCB and is the main Brazilian rocket launching center. In the meteorological facility at CLA, surface and upper-air data are collected on a routine basis (Marques and Fisch 2005). Radiosondes are launched daily at 1200 UTC (also at 0000 UTC in recent years), and the collected data are representative of an area of approximately 250 km × 250 km centered at the CLA (WMO 2010). Over the CLA region, the frequency of SL occurrence is higher from February to July (>5 cases per month; Barros and Oyama 2010). The specific month of July is chosen here to avoid the association between SLs and ITCZ (Fig. 3). In July, the ITCZ is located far north of the CLA region (at ~7°N; Melo et al. 2009) and does not directly affect the SL initiation over the NCB. Therefore, the present work focuses on the SL initiation that is not related to the strong synoptic forcing (low-level atmospheric convergence) induced by the ITCZ.

The method for obtaining the antecedent conditions related to SL initiation consists of comparing the mid-morning average atmospheric conditions between days with SLs and without organized deep convection in the following late afternoon or early evening. Because the identification of SLs is usually carried out subjectively from satellite images (e.g., Cavalcanti 1982; Cohen et al. 1989, 2009), differences in the classification of the days are likely to occur. To minimize this uncertainty, an

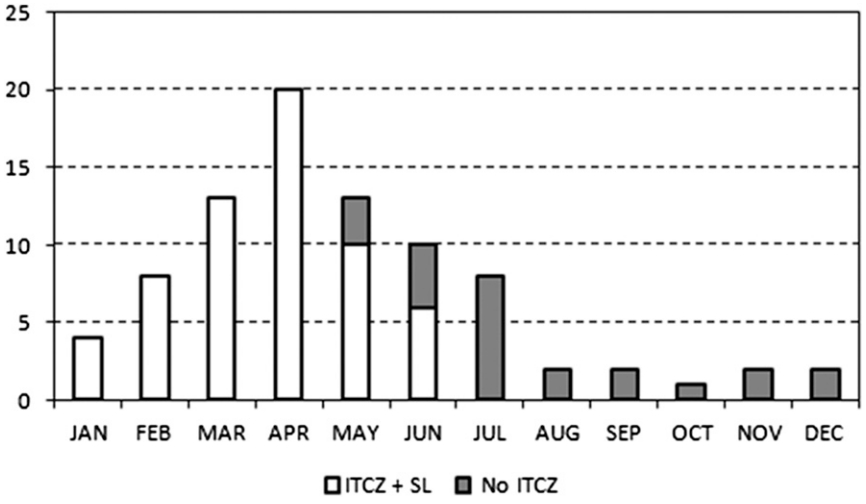

FIG. 3. Average frequency of SLs (cases per month) over the CLA region from 2005 to 2006. The number of cases related (unrelated) to the ITCZ is in white (gray) and referred to as ITCZ + SL (No ITCZ). For instance, in June, the total number of cases is 10 (cases per month), and 6 are related to the ITCZ; in July, all 8 cases are not related to the ITCZ. [Adapted from Barros and Oyama (2010) and Barros (2008).]

objective method is developed to identify the SLs. The method is based on the morphological properties of the convective systems that occur over the NCB in the late afternoon or early evening.

This work, therefore, aims to 1) objectively identify the SLs that initiate in July over the CLA region and 2) obtain the antecedent atmospheric conditions related to SL initiation. In the next section (section 2), the data and methodology, including the objective method, are described. In section 3, the results from the objective method are presented, and its accuracy is evaluated. The antecedent atmospheric conditions related to SL initiation are presented in section 4. Concluding remarks are presented in section 5.

2. Data and methodology

a. Convection categories

According to the deep convection and cloudiness features over the NCB in the late afternoon or early morning, each day in July is classified in one of the following three categories:

- no-convection category (NOC), if deep convection occurs in a sparse or isolated manner (Fig. 1b);
- squall-line category (SLC), if SL occurs, that is, the convective systems are organized linearly as an SL (Fig. 1a); and
- coastal convection category, if deep convection does occur but it is neither isolated nor linearly organized (Fig. 1c).

The classification is carried out both objectively and subjectively. The objective method is described in the following subsection.

b. Objective method

The morphological properties of the convective systems diagnosed from infrared satellite images by the Forecast and Tracking the Evolution of Cloud Clusters (ForTraCC; Vila et al. 2008) software are the input of the objective method. ForTraCC has run operationally at the Brazilian Center for Weather Forecasting and Climate Research (CPTEC) since 2004. In this study, data for the month of July over the course of 9 years, from 2004 to 2012, are used.

For each day in July, the objective method selects the convective systems that occur over the coastal region from the city of Belém to the CLA (box area in Fig. 2) between 1800 and 0100 UTC (1500 and 2200 LST). Based on the morphological properties of the selected convective systems, such as area, size, and shape, the day is classified in the NOC, SLC, or coastal convection category according to the algorithm shown in Fig. 4. For July months from 2004 to 2012, the objective and subjective classifications are compared in section 3. The subjective classification was provided by Oliveira (2012) and follows the criteria given in Cavalcanti (1982).

c. Atmospheric variables

Two distinct datasets are used to obtain the atmospheric conditions at 1200 UTC in July for the period from 2004 to 2012:

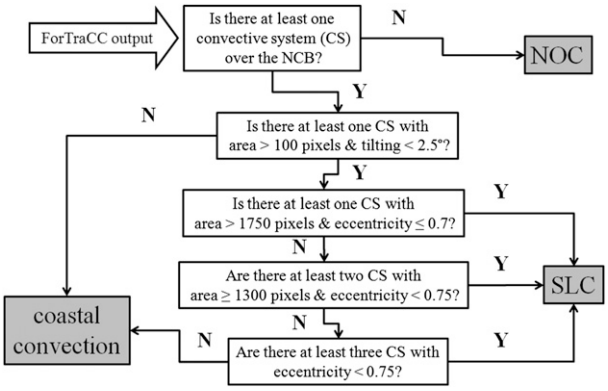

FIG. 4. Algorithm of the objective method. For each 15-min period from 1800 to 0100 UTC, from the ForTraCC output, the period is classified into one of the three convection categories (SLC, NOC, or the coastal convection category). A day is classified as being in NOC (SLC) if all periods (at least one period) are (is) classified in NOC (SLC). If a day is not classified in NOC or SLC, it is classified in the coastal convection category. A pixel refers to a 4 km × 4 km area. Eccentricity tends to 1 (0) for circular (linear) shapes. For noncircular convective system, tilting refers to the angle between the major axis of the convective system and the zonal direction (positive in the counterclockwise direction); for circular convective system, tilting is equal to 0.

- upper-air data from the daily radiosonde launchings at CLA and
- gridded data (1.5° × 1.5°) from ERA-Interim (Dee et al. 2011).

To obtain the antecedent conditions related to SL initiation, the average of SLC is compared to the average of NOC for several variables contained in these datasets. We shall also consider that SLC and NOC are composed of the days for which there is agreement between the objective and subjective classifications. For the atmospheric column over the CLA region, the statistical significance of the differences between SLC and NOC is evaluated by a Student's t test at the 99% level.

3. Objective method results

The results of the objective method are compared to the subjective identification provided by Oliveira (2012). The results are given first for SLC and then for NOC.

For SLC, the objective method systematically identifies more cases than the subjective method (Fig. 5a): on average, nine cases per month are identified objectively and seven cases per month are found subjectively. This difference can be regarded as small (Oliveira 2012); therefore, the objective and subjective classifications are in good agreement.

The comparison of the dates when the SLCs are identified is summarized in the contingency table shown in Table 1, and the contingency table measures are given in appendix A. The hit rate of the objective method is high (92%), but the false alarm ratio is also substantial (29%). The overestimation of the objective method also reflects the bias, which is equal to 1.3. Therefore, the objective method is able to identify almost all SLs identified subjectively, but identifies more cases. The overall accuracy of the objective method, measured by the critical success index (CSI; or threat score), is good (CSI = 0.67; i.e., ~2/3).

For the NOC, the objective method also systematically identifies more cases than does the subjective method (Fig. 5b). On average, the difference of about one case per month is found, and this overestimation reflects the bias, which is ~1.1 (Table 2). The objective method is able to identify almost all cases of NOC (with a hit rate of 90%), but identifies additional cases (with a false alarm ratio of 21%). The overall accuracy of the objective method is good (CSI = 0.72). Therefore, for SLC and NOC, the accuracy and errors of the objective method are similar.

To compute the average of SLC and NOC, as mentioned earlier (section 2), we shall consider only the cases for which there is agreement between the objective and subjective classifications. Under this criterion, the average frequency of SLC is about six cases per month in July, and the average frequency of NOC is about eight cases per month (represented by black bars in Fig. 5). These frequencies are similar to those obtained subjectively, because the hit rate of the objective method is high.

4. Antecedent conditions related to SL initiation

a. *Vertical profile*

For SLC and NOC, the average values of two instability indices, K index (IK) and total totals index (ITT) over the CLA region at 1200 UTC (0900 LST) are shown in Table 3 (the definitions of these indices are given in appendix B). IK and ITT depend on the thermodynamic conditions of the vertical profile and assess the probability of deep convection occurrence. Both indices are higher for SLC, and the difference between the categories is statistically significant. Therefore, the SL initiation (in the late afternoon or early evening) is preceded by the occurrence of conditions more favorable to convective storms at midmorning.

The average vertical profiles of the zonal wind for SLC and NOC are similar (Figs. 6a,b): nearly constant easterly winds in the low and midlevels, and westerly winds in the upper levels. Because of the similarity among the profiles, the differences are not significant for all levels. Therefore, the zonal wind might not be related

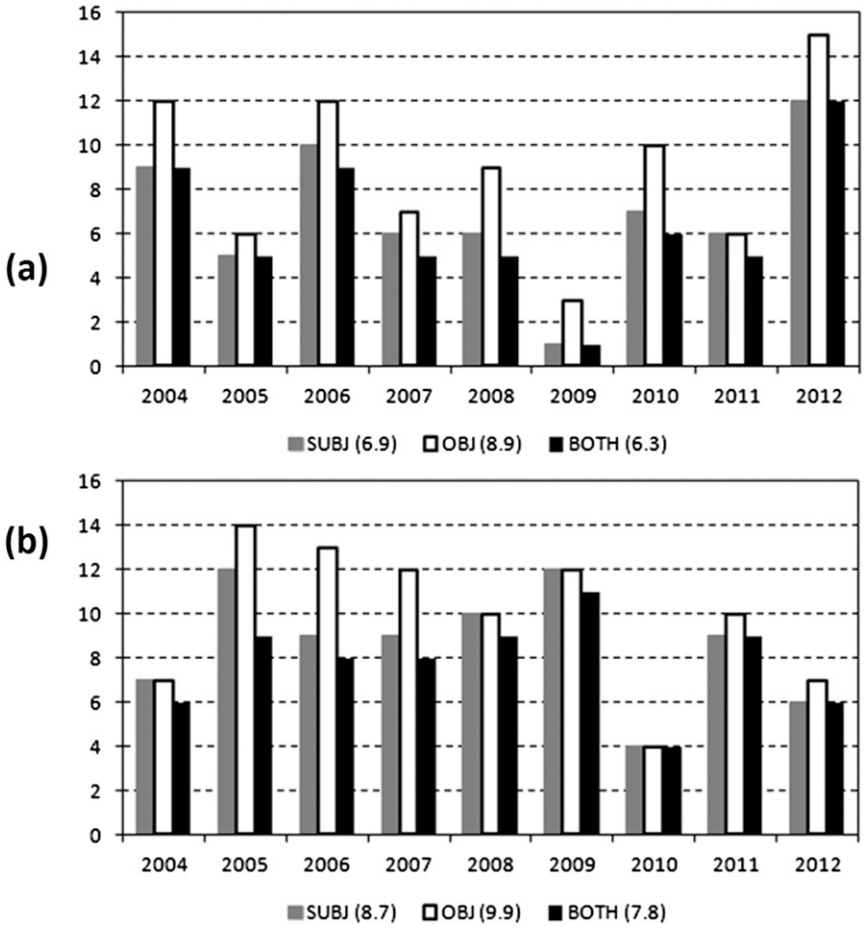

FIG. 5. (a) Frequency of SLCs in July (cases per month) from 2004 to 2012 identified by the objective (OBJ; white bars), subjective (SUBJ; gray bars), or both methods (BOTH; black bars). The value in parentheses refers to the average frequency (cases per month). (b) As in (a), but for NOC.

to SL initiation. For the lower levels (below 750 hPa), this could be partially the result of averaging more and less intense low-level zonal jets related to propagating and nonpropagating SLCs, respectively (Cohen 1996; Alcântara et al. 2011).

The average vertical profiles of the meridional wind show clear differences between SLC and NOC at some levels (Figs. 6c,d). The profiles are similar in the low and midlevels; in the upper levels, northerly (southerly) wind is found for SLC (NOC). At 350 hPa, the difference is statistically significant for both datasets (radiosonde and reanalysis data): for NOC, an almost easterly flow occurs (because the meridional wind is almost zero); for SLC, the atmospheric flow veers toward the northeasterly direction (because a substantial northerly component is added to the easterly flow). An explanation of the relation between this circulation difference at 350 hPa and SL initiation is given in the next subsection.

TABLE 1. Contingency table for the comparison of dates when an SLC is identified by the objective and subjective methods. Yes means that an SLC is identified.

		Subjective method	
		Yes	No
Objective method	Yes	57	23
	No	5	194

TABLE 2. Contingency table for the comparison of dates when an NOC is identified by the objective and subjective methods. Yes means that an NOC is identified.

		Subjective method	
		Yes	No
Objective method	Yes	70	19
	No	8	182

TABLE 3. Average plus or minus one std dev of two instability indices (IK and ITT) for SLC and NOC, computed from the radiosonde and reanalysis data. For both indices, the difference between the average values of SLC and NOC is statistically significant at the 99% level.

	Reanalysis data		Radiosonde data	
Index	SLC	NOC	SLC	NOC
IK	28.8 ± 3.6	20.2 ± 5.7	29.0 ± 4.9	19.5 ± 8.0
ITT	41.1 ± 1.9	38.4 ± 2.2	42.0 ± 2.9	33.2 ± 7.7

The average vertical profiles of dewpoint depression show that, for SLC, the layer between 850 and 350 hPa is significantly wetter for both datasets (Figs. 6e,f). Therefore, instability indices that depend on the moisture content in this layer, such as the IK and ITT, could also show significant differences between the categories; this is indeed the case, as shown previously. Moreover, the fact that a wetter layer between 850 and 350 hPa at midmorning precedes the SL initiation is consistent with studies that consider the moisture content above the planetary boundary layer to be the key factor in the transition from shallow to deep convective clouds (Holloway and Neelin 2009; Derbyshire et al. 2004; Zhang and Klein 2010).

b. *Large-scale factors*

In the previous section, it was shown that some features of the vertical profile over the CLA region at 1200 UTC, high moisture content at low and midlevels and northeasterly flow at upper levels, are related to subsequent SL initiation in the late afternoon or early evening. In this section, the horizontal fields of these variables at 1200 UTC are analyzed using the reanalysis data. The average fields of SLC and NOC are compared, similarly to what was done in the previous section. The dewpoint depression at 700 hPa and the atmospheric circulation at 350 hPa are addressed, because significant differences between the categories for both datasets (radiosonde and reanalysis data) were found in these variables over the CLA region. For the moisture content, the level of 700 hPa is chosen because humidity at this level plays an important role in shaping the annual cycle of precipitation for the CLA region (Oliveira and Oyama 2009).

At 1200 UTC, the monthly average dewpoint depression field at 700 hPa in July (Fig. 7a) shows high moisture content (depression $<10°C$) over the regions under the direct influence of the ITCZ: northern South America, the equatorial Atlantic Ocean, and central Africa. The CLA region lies in the transition zone between the wetter conditions over the ITCZ and northwestern Amazonia, and the drier conditions over central and eastern Brazil related to the South Atlantic subtropical high. These features are consistent with the precipitation climatology for the austral winter (e.g., Garreaud and Aceituno 2007). For SLC and NOC, the spatial pattern of the dewpoint depression (not shown) is in general similar to the monthly average field, but a clear dipole pattern of moister NCB and drier southeastern South America emerges when the difference between these categories is computed (Fig. 7b). This dipole pattern could be viewed as a direct circulation cell, with moister (drier) conditions over equatorial (subtropical) latitudes due to moisture convergence (divergence) anomalies, and it resembles the precipitation anomalies during La Niña events (e.g., Ropelewski and Halpert 1989; Coelho et al. 2002). Therefore, antecedent conditions (at 1200 UTC) that are moister over NCB and/or drier over southeastern South America are favorable to the subsequent SL initiation. These conditions may also result from transient systems that occur in July, such as easterly waves (which bring more moisture for the NCB; Coutinho and Fisch 2007) and warm and dry spells in austral winter over central South America (Satyamurty et al. 2007). Preliminary results (not shown) suggest that these systems do not necessarily affect the SL initiation, but could be important for specific cases.

The monthly average circulation at 350 hPa in July consists of an easterly flow over the NCB (Fig. 8a). It belongs to the northern branch of a zonally oriented anticyclonic circulation that extends from South America to Africa (the southern branch is linked at ~15°S to the strong westerly flow in the Southern Hemisphere). These features agree with the upper-level circulation climatology for the austral winter (e.g., Molion 1987; Garreaud and Aceituno 2007). Two cores (closed circulation) are found within the anticyclonic circulation region: one over Amazonia and the other over the Atlantic Ocean close to northeastern Brazil (labeled with the letter A in Fig. 8). For SLC, the A center is more intense; for NOC, it is less intense (Figs. 8b,c). Higher intensity means more horizontal (zonal and/or meridional) extension and/or higher vorticity magnitude, and the circulation over the NCB veers toward the northeasterly direction; that is, a northerly wind component emerges over the NCB. Therefore, higher (lower) positive vorticity at 350 hPa over the NCB is an antecedent condition favorable (unfavorable) to subsequent SL initiation.

For SLC, the positive vorticity anomalies at 350 hPa (and related wind veering) could be viewed as the upper-level response of low-level convergence anomalies. For instance, at 850 hPa, pronounced atmospheric convergence anomalies are found along the NCB (not shown). This midmorning low-level convergence anomaly is a favorable condition for the subsequent development of

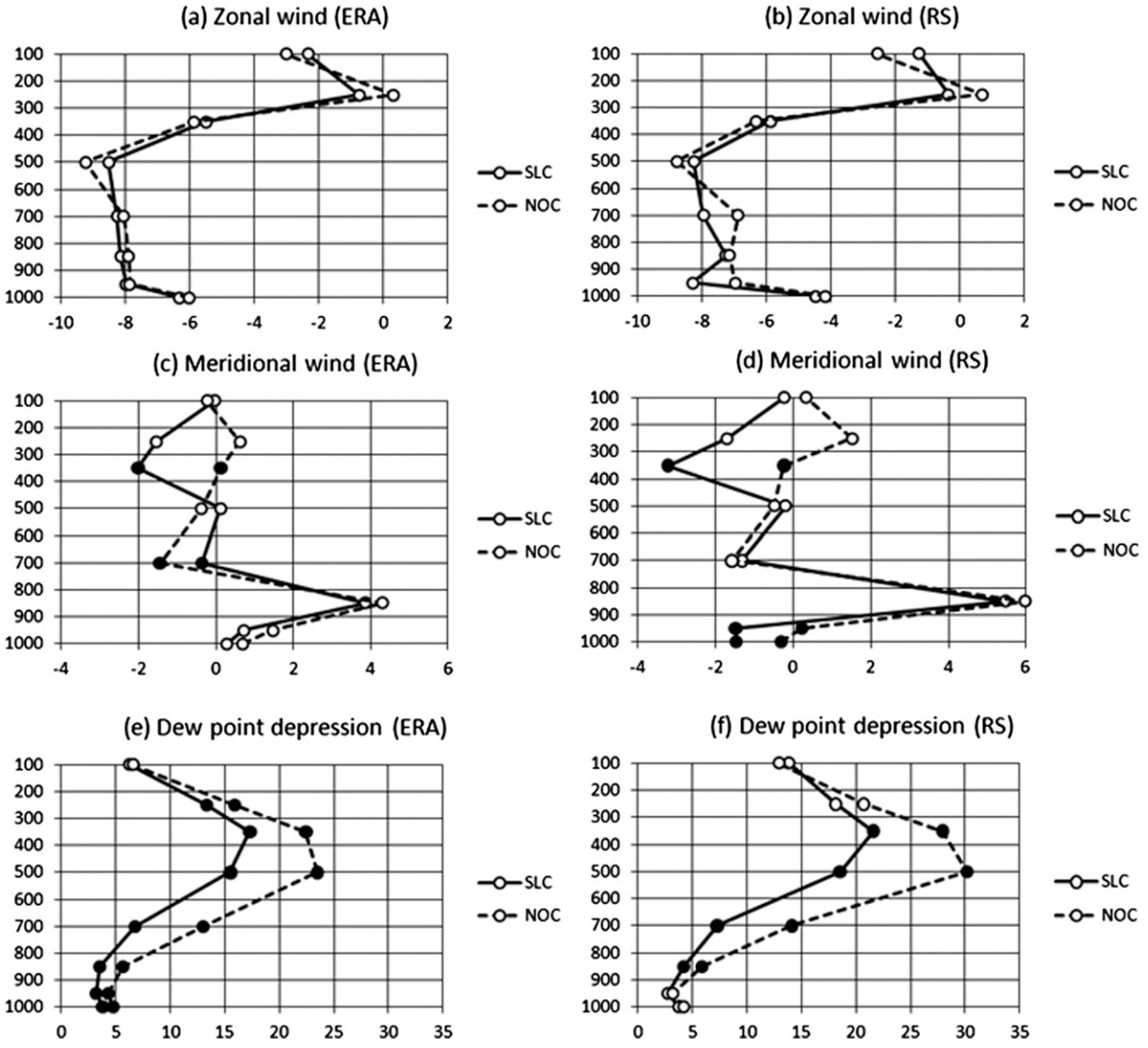

FIG. 6. Average vertical profiles of (a),(b) zonal wind ($m\,s^{-1}$); (c),(d) meridional wind ($m\,s^{-1}$); and (e),(f) dewpoint depression (°C) for SLC and NOC. The vertical axis refers to pressure levels (hPa). Profiles are computed from the (left) reanalysis (ERA) and (right) radiosonde (RS) data. Filled circles are plotted at the levels where the difference of the average values between SLC and NOC is statistically significant at the 99% level.

deep convection and sea breeze, which are important processes related to SL initiation.

5. Concluding remarks

The antecedent atmospheric conditions at 1200 UTC (0900 LST) related to subsequent SL initiation in the late afternoon or early evening over the NCB were obtained for a specific month, July, for 9 years (from 2004 to 2012). This month was chosen to focus on SL initiation that is independent from the strong synoptic forcing (low-level atmospheric convergence) related to the ITCZ (which occurs in the austral autumn). An objective method, based on the morphological properties of the convective systems that occur over the NCB in the late afternoon or early evening, was developed to aid in the classification of each day in July in one of the three categories: SLC (if an SL initiates), NOC (if deep convection is isolated or sparse), or the coastal convection category (if deep convection occurs, but it is neither isolated nor linearly organized). For SLC and NOC, the objective method showed good accuracy when compared to the subjective identification provided by Oliveira (2012).

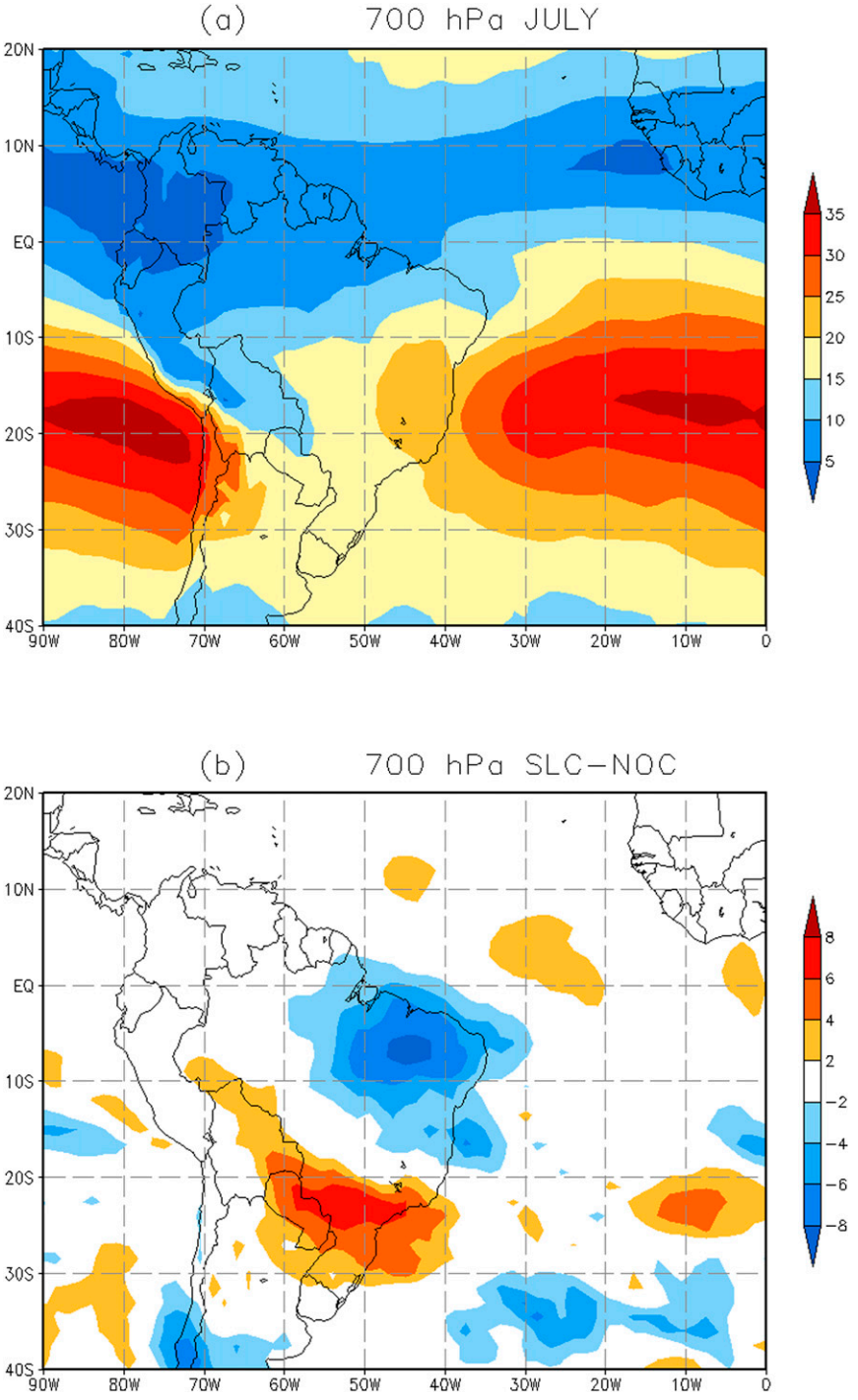

FIG. 7. (a) Average dewpoint depression at 700 hPa in July (°C). (b) Difference in the average dewpoint depression at 700 hPa between SLC and NOC (SLC minus NOC; °C).

SLC and NOC were composed of the cases (days) for which there was agreement between the objective and subjective classifications. Under this criterion, the average frequency was six cases per month for SLC and eight cases per month for NOC. The statistically significant differences between the average of SLC and NOC were used to characterize the midmorning atmospheric conditions favorable to subsequent SL initiation.

For a specific region in the NCB, the CLA region, the vertical profiles for SLC and NOC, computed from

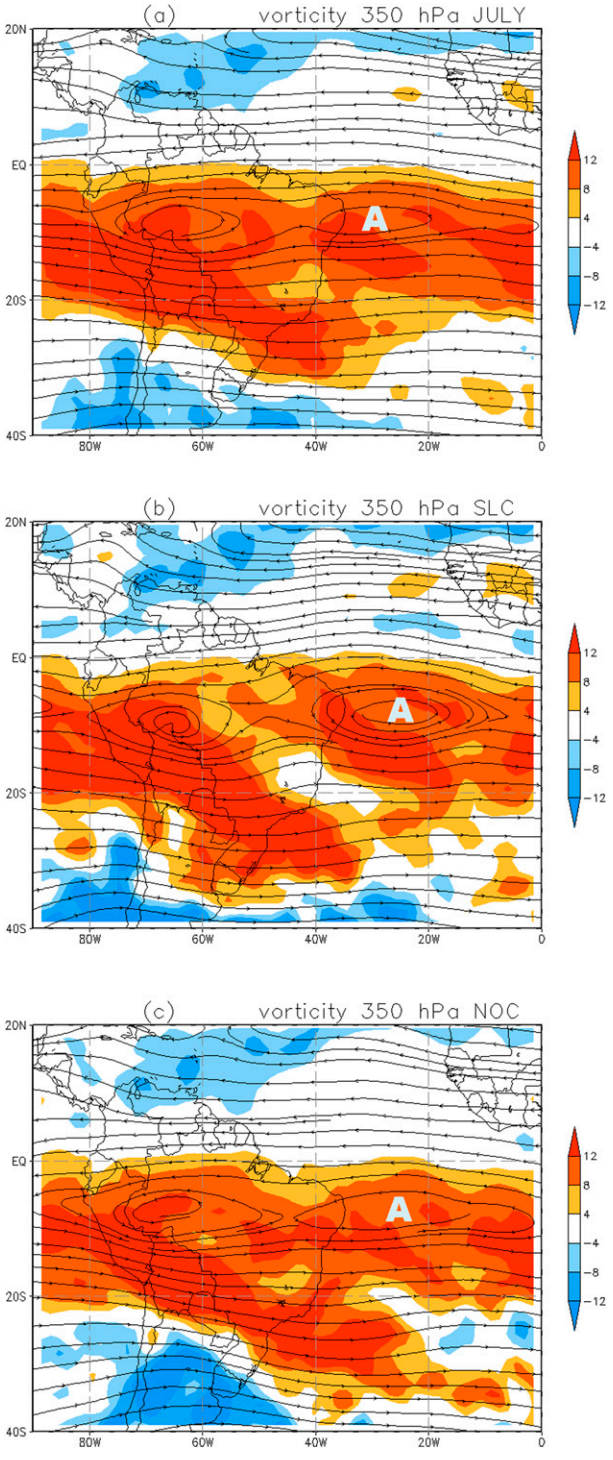

FIG. 8. (a) Streamlines of the average circulation at 350 hPa in July. (b) As in (a), but for SLC. (c) As in (a), but for NOC. The letter A indicates the position of the anticyclonic center over the Atlantic Ocean close to northeastern Brazil. Shading refers to the vorticity (10^{-6} s^{-1}).

radiosonde and ERA-Interim, were compared. By focusing on the significant differences for both datasets, it was found that two midmorning conditions are favorable for SL initiation: a moister layer between 850 and 350 hPa, and a northeasterly flow at 350 hPa. The moister layer was also related to a higher probability of convective storm occurrence, as indicated by the higher values of the *K* and total totals indices. These conclusions were quite robust, because they were valid for two independent datasets (radiosonde and reanalysis data).

Using the reanalysis data, the horizontal fields of SLC and NOC for the dewpoint depression at 700 hPa and atmospheric circulation at 350 hPa were compared. It was found that moister (drier) conditions over the whole NCB (southeastern South America) at 700 hPa and more intense anticyclonic circulation over the Atlantic Ocean close to northeastern Brazil at 350 hPa are antecedent conditions that favor SL initiation. These conditions might be the result of an anomalous direct meridional cell and, for specific cases, the action of transient systems such as easterly waves and/or dry spells over central South America.

The findings reported here have the potential to aid weather forecasting activities. A preliminary attempt in this regard was made by Oyama and Oliveira (2013), who showed that, by using the midmorning values of dewpoint depression at 700 hPa and meridional wind at 350 hPa as predictors, approximately ⅔ of the NOCs and ½ of the SLCs could be predicted 6–12 h ahead by a simple algorithm. These results are lower than but comparable to the hit rates of short-term thunderstorm prediction models found in the literature (e.g., Ravi et al. 1999; Manzato 2005; Kunz 2007), and they could be improved by including variables that represent the activity of quasi-stationary systems (such as the dry spells over central South America) and numerical weather prediction products, or by using advanced statistical methods. These aspects will be addressed in future studies.

Acknowledgments. This work is part of FPO's M.S. dissertation under the guidance of MDO. FPO was supported by a grant from the Brazilian National Council for Scientific and Technological Development (CNPq). The authors are grateful to the three anonymous reviewers and to the editor (Mr. Philip N. Schumacher) for their useful comments.

APPENDIX A

Contingency Table Measures

The 2 × 2 contingency table given below (Table A1) is used to verify the ability of the objective method in

TABLE A1. General form of the 2 × 2 contingency tables shown in Tables 1 and 2. Yes (No) refers to the cases that are (are not) identified by the method.

		Subjective method	
		Yes	No
Objective method	Yes	*a*	*b*
	No	*c*	*d*

identifying SLCs and NOCs. The number in each cell has a definite meaning: *a* refers to hits, *b* to false alarms, *c* to misses, and *d* to correct rejections. If the objective method is able to reproduce all the results from the subjective method, then $b = c = 0$.

The definitions of the contingency table measures mentioned in the text—bias *B*, hit rate *H*, false alarm rate (FAR), and critical success index (CSI; or threat score)—are is given below (Wilks 2006):

$$B = \frac{a+b}{a+c},$$

$$H = \frac{a}{a+c},$$

$$\text{FAR} = \frac{b}{a+b}, \quad \text{and}$$

$$\text{CSI} = \frac{a}{a+b+c}.$$

APPENDIX B

Instability Indices

The definitions of the instability indices mentioned in the text—*K* index (IK) and total totals index (ITT)—are given below (e.g., Peppler 1988):

$$\text{IK} = T_{850} - T_{500} + T_{d_{850}} - \text{Dep}_{700} \quad \text{and}$$

$$\text{ITT} = T_{850} + T_{d_{850}} - 2T_{500},$$

where T is the temperature, T_d is the dewpoint temperature, Dep is the dewpoint depression (i.e., $T - T_d$), and the numerical subscripts refer to the pressure levels (hPa).

REFERENCES

Alcântara, C. R., M. A. F. Silva Dias, E. P. Souza, and J. C. P. Cohen, 2011: Verification of the role of the low level jets in Amazon squall lines. *Atmos. Res.*, **100**, 36–44, doi:10.1016/j.atmosres.2010.12.023.

Barros, S. S., 2008: Precipitação no Centro de Lançamento de Alcântara: Aspectos observacionais e de modelagem (Rainfall at the Alcântara Rocket Launching Center: Observational and modeling aspects). M.S. thesis, National Institute for Space Research, São José dos Campos, São Paulo, Brazil, 112 pp. [Available online at http://urlib.net/sid.inpe.br/mtc-m18@80/2008/07.11.13.43.]

——, and M. D. Oyama, 2010: Sistemas Meteorológicos Associados à Ocorrência de Precipitação no Centro de Lançamento de Alcântara (Rainfall at the Alcântara Rocket Launching Center: Observational and modeling aspects). *Rev. Bras. Meteor.*, **25**, 333–344, doi:10.1590/S0102-77862010000300005.

Cavalcanti, I. F. A., 1982: Um estudo sobre interações entre sistemas de circulação de escala sinótica e circulações locais (A study of the interactions between synoptic and local circulations). M.S. thesis, National Institute for Space Research, São José dos Campos, São Paulo, Brazil, 140 pp. [Available online at http://urlib.net/6qtX3pFwXQZGivnJSY/HfD3p.]

Coelho, C. A. S., C. B. Uvo, and T. Ambrizzi, 2002: Exploring the impacts of the tropical Pacific SST on the precipitation patterns over South America during ENSO periods. *Theor. Appl. Climatol.*, **71**, 185–197, doi:10.1007/s007040200004.

Cohen, J. C. P., 1996: Mecanismos de propagação das linhas de instabilidade na Amazônia (Mechanisms related to squall line propagation over Amazonia). Ph.D. thesis, University of São Paulo, 173 pp.

——, M. A. F. Silva Dias, and C. A. Nobre, 1989: Aspectos climatológicos das linhas de instabilidade na Amazonia (Climatological features of squall lines over Amazonia). *Climanálise*, **4**, 34–40.

——, ——, and ——, 1995: Environmental conditions associated with Amazonian squall lines: A case study. *Mon. Wea. Rev.*, **123**, 3163–3174, doi:10.1175/1520-0493(1995)123<3163:ECAWAS>2.0.CO;2.

——, I. F. A. Cavalcanti, R. H. M. Braga, and L. Santos Neto, 2009: Linhas de Instabilidade na costa N-NE da América do Sul (Squall lines over the north-northeast coast of South America). *Tempo e Clima no Brasil*, I. F. A. Cavalcanti et al., Eds., Oficina de Textos, 75–93.

Coutinho, E. C., and G. Fisch, 2007: Distúrbios Ondulatórios de Leste (DOLs) na Região do Centro de Lançamento de Alcântara-MA [Easterly wave disturbance (DOLs) at the region of Alcântara Launching Center-MA]. *Rev. Bras. Meteor.*, **22**, 193–203, doi:10.1590/S0102-77862007000200005.

Dee, D. P., and Coauthors, 2011: The ERA-Interim reanalysis: Configuration and performance of the data assimilation system. *Quart. J. Roy. Meteor. Soc.*, **137**, 553–597, doi:10.1002/qj.828.

Derbyshire, S. H., I. Beau, P. Bechtold, J.-Y. Grandpeix, J.-M. Piriou, J.-L. Redelsperger, and P. M. M. Soares, 2004: Sensitivity of moist convection to environmental humidity. *Quart. J. Roy. Meteor. Soc.*, **130**, 3055–3079, doi:10.1256/qj.03.130.

Garreaud, R. D., and P. Aceituno, 2007: Atmospheric circulation over South America: Mean features and variability. *The Physical Geography of South America*, T. Veblen, K. Young, and A. Orme, Eds., Oxford University Press, 45–66.

Garstang, M., H. L. Massie Jr., J. Halverson, S. Greco, and J. Scala, 1994: Amazon coastal squall lines. Part I: Structure and kinematics. *Mon. Wea. Rev.*, **122**, 608–622, doi:10.1175/1520-0493(1994)122<0608:ACSLPI>2.0.CO;2.

Greco, S., and Coauthors, 1990: Rainfall and surface kinematic conditions over central Amazonia during ABLE 2B. *J. Geophys. Res.*, **95**, 17 001–17 014, doi:10.1029/JD095iD10p17001.

Holloway, C. E., and J. D. Neelin, 2009: Moisture vertical structure, column water vapor, and tropical deep convection. *J. Atmos. Sci.*, **66**, 1665–1683, doi:10.1175/2008JAS2806.1.

Houze, R. A., Jr., 2004: Mesoscale convective systems. *Rev. Geophys.*, **42**, RG4003, doi:10.1029/2004RG000150.

Kousky, V. E., 1980: Diurnal rainfall variation in northeast Brazil. *Mon. Wea. Rev.*, **108**, 488–498, doi:10.1175/1520-0493(1980)108<0488:DRVINB>2.0.CO;2.

Kunz, M., 2007: The skill of convective parameters and indices to predict isolated and severe thunderstorms. *Nat. Hazards Earth Syst. Sci.*, **7**, 327–342, doi:10.5194/nhess-7-327-2007.

Manzato, A., 2005: The use of sounding-derived indices for a neural network short-term thunderstorm forecast. *Wea. Forecasting*, **20**, 896–917, doi:10.1175/WAF898.1.

Marques, R. F. C., and G. F. Fisch, 2005: As atividades de Meteorologia Aeroespacial no Centro Técnico Aeroespacial (CTA) [The activities of Aerospace Meteorology in the Aerospace Technical Center (CTA)]. *Bol. Soc. Bras. Meteor.*, **29**, 21–25.

Melo, A. B. C., I. F. A. Cavalcanti, and P. P. Souza, 2009: Zona de Convergência Intertropical do Atlântico (Atlantic intertropical convergence zone). *Tempo e Clima no Brasil*, I. F. A. Cavalcanti et al., Eds., Oficina de Textos, 25–41.

Molion, L. C. B., 1987: Climatologia dinâmica da região Amazônica: Mecanismos de precipitação. *Rev. Bras. Meteor.*, **2**, 107–117.

——, and S. O. Bernardo, 2002: Uma revisão da dinâmica das chuvas no nordeste brasileiro (A review of rainfall dynamics over northeastern Brazil). *Rev. Bras. Meteor.*, **17**, 1–10.

Oliveira, F. P., 2012: Fatores associados à iniciação de linhas de instabilidade na região do Centro de Lançamento de Alcântara no mês de julho (Conditions related to squall line initiation in the Alcântara Launch Center region in July). M.S. thesis, National Institute for Space Research, São José dos Campos, São Paulo, Brazil, 99 pp. [Available online at http://urlib.net/8JMKD3MGP8W/3BATESB.]

——, and M. D. Oyama, 2009: Radiosounding-derived convective parameters for the Alcântara Launch Center. *J. Aerosp. Technol. Manage.*, **1**, 211–216, doi:10.5028/jatm.2009.0102211216.

Oyama, M. D., and F. P. Oliveira, 2013: Prediction of squall line occurrence over the Alcântara Launch Center in July. *Proc. V Simpósio Internacional de Climatologia*, Florianópolis, Brazil, Sociedade Brasileira de Meteorologia. [Available online at http://sic2013.web2105.uni5.net/inexx/anais.]

Peppler, R. A., 1988: A review of static stability indices and related thermodynamic parameters. SWS Misc. Publ. 104, Climate and Meteorology Section, Illinois State Water Survey Division, Illinois Department of Energy and Natural Resources, 87 pp. [Available online at http://www.isws.illinois.edu/pubdoc/MP/ISWSMP-104.pdf.]

Ravi, N., U. C. Mohanty, O. P. Madan, and R. K. Paliwal, 1999: Forecasting of thunderstorms in the pre-monsoon season at Dehli. *Meteor. Appl.*, **6**, 29–38, doi:10.1002/met.19996103.

Reboita, M. S., M. A. Gan, R. P. da Rocha, and T. Ambrizzi, 2010: Regimes de precipitação na América do Sul: Uma revisão bibliográfica (Precipitation regimes in South America: A bibliography review). *Rev. Bras. Meteor.*, **25**, 185–204, doi:10.1590/S0102-77862010000200004.

Ropelewski, C. F., and M. S. Halpert, 1989: Precipitation patterns associated with the high index phase of the Southern Oscillation. *J. Climate*, **2**, 268–284, doi:10.1175/1520-0442(1989)002<0268:PPAWTH>2.0.CO;2.

Satyamurty, P., M. S. Teixeira, and C. K. Padilha, 2007: Warm and dry spells (WDS) in austral winter over central South America. *Ann. Geophys.*, **25**, 1049–1069, doi:10.5194/angeo-25-1049-2007.

Vila, D. B., L. A. T. Machado, H. Laurent, and I. Velasco, 2008: Forecast and Tracking the Evolution of Cloud Clusters (ForTracCC) using satellite infrared imagery: Methodology and validation. *Wea. Forecasting*, **23**, 233–245, doi:10.1175/2007WAF2006121.1.

Wilks, D. S., 2006: *Statistical Methods in the Atmospheric Sciences.* Academic Press, 627 pp.

World Meteorological Organization, 2010: Manual on the Global Observing System. Volume I: Global aspects. WMO 544, 62 pp. [Available online at http://www.wmo.int/pages/prog/www/OSY/Manuals_GOS.html.]

Zhang, Y., and S. A. Klein, 2010: Mechanisms affecting the transition from shallow to deep convection over land: Inferences from observations of the diurnal cycle collected at the ARM Southern Great Plains site. *J. Atmos. Sci.*, **67**, 2943–2959, doi:10.1175/2010JAS3366.1.